AGU PUBLICATIONS

JGR

Journal of Geophysical Research: Atmospheres

RESEARCH ARTICLE
10.1002/2015JD023206

**Key Points:**
- The soil moisture obviously decreased from 1948 to 2010 over East Asia
- Decreasing precipitation is a major reason in triggering the soil drying
- Soil drying is enhanced almost twofold by increasing temperature

**Correspondence to:**
J. Huang,
hjp@lzu.edu.cn

**Citation:**
Cheng, S., X. Guan, J. Huang, F. Ji, and R. Guo (2015), Long-term trend and variability of soil moisture over East Asia, *J. Geophys. Res. Atmos.*, *120*, doi:10.1002/2015JD023206.

Received 3 FEB 2015
Accepted 8 JUN 2015
Accepted article online 10 JUN 2015



# Long-term trend and variability of soil moisture over East Asia

**Shanjun Cheng[1], Xiaodan Guan[1], Jianping Huang[1], Fei Ji[1], and Ruixia Guo[1]**

[1]Key Laboratory for Semi-Arid Climate Change of the Ministry of Education, College of Atmosphere Sciences, Lanzhou University, Lanzhou, China

**Abstract** The variability of soil moisture over East Asia was analyzed using a long-term data set from the Global Land Data Assimilation System. Overall, a clear decreasing trend occurred over a period of 63 years, with pronounced drying over northeast China, north China, part of Mongolia, and Russia near lake Baikal. Statistical analyses show that decreasing precipitation and global warming have different effects on the decrease in soil moisture. The qualitative analysis and quantitative contributions illustrated that soil drying is driven primarily by decreasing precipitation and is enhanced almost twofold by increasing temperatures. As soil moisture decreases, the positive feedback between soil moisture and temperature may result in future water shortages. Following the Representative Concentration Pathways 8.5 (RCP8.5) and 4.5 (RCP4.5) simulation scenarios of Coupled Model Intercomparison Project phase 5, the model-predicted soil moisture demonstrated a continuously decreasing trend during the 21st century.

## 1. Introduction

Soil moisture plays an important role in modifying the behavior of atmosphere by its influence on land surface fluxes of moisture, energy, carbon, and trace gases [*Seneviratne et al*., 2010]. As a key factor in the water cycle, soil moisture is closely associated with precipitation and evapotranspiration, which include mainly plant transpiration and bare soil evaporation [*Hohenegger et al*., 2009; *Wetzel and Chang*, 1987]. It also takes part in the energy cycle by changing soil thermal parameters and surface albedo [*Nakshabandi and Kohnke*, 1965; *Teuling and Seneviratne*, 2008], via its impact on the partitioning of incoming energy into latent and sensible heat fluxes [*Bastiaanssen*, 2000]. Furthermore, soil moisture strongly interacts with the biosphere by affecting the terrestrial carbon exchange and nitrogen cycle [*Fierer and Schimel*, 2002; *Granier et al*., 2007]. As the immediate water source, vegetation is sensitive to the variability of soil moisture. Extreme drought or drying is often accompanied by changes in vegetation productivity and species [*Ciais et al*., 2005; *Reichstein et al*., 2007]. Therefore, studying soil moisture and its variation, especially its variability under global warming, is crucial to understanding climate change and land-atmosphere interaction.

Traditionally, soil moisture change and its interaction with the Earth system have been studied with ground-based measurements [*Brocca et al*., 2011; *Guan et al*., 2009; *Huang et al*., 2008; *Wang et al*., 2010]. However, as in situ observations are commonly scarce and limited in space and time, most current studies focus on the variability of soil moisture and its related hydrological variation in larger spatial domains or over long time scales that are mainly based on the outputs of remote sensing, model simulations [*Yang et al*., 2011], and data assimilations [*Yang et al*., 2009, 2007]. Despite the use of different types of data sets, some common features of soil moisture change have been captured, especially the drying across East Asia [*Dai*, 2013; *Dorigo et al*., 2012; *Li et al*., 2014]. East Asia, as one of the world's most populous regions, is sensitive to climate change with diverse land surface cover and fragile ecosystems [*Huang et al*., 2010, 2014]. Drying over East Asia is more severe than over other regions and extremely urgent to mitigate. However, the explanation for this drying remains unclear because of its complexity and dependence on a variety of mechanisms, such as the interactions with climate change, biosphere evolution, and human activities. The sensibility of soil moisture and feedback with environment variables among different land surfaces are different, even contrary, which makes investigation of these mechanisms in the real world more difficult.

In this paper, we investigate the trend and variability of soil moisture in East Asia over the second half of the 20th century. The analysis is based on data sets derived from the Global Land Data Assimilation System (GLDAS), which is a multimodel simulation system that provides fundamental long-term information about

land surface processes and interactions between the land surface and the atmosphere from regional to global scales [*Rodell et al*., 2004]. The forcing mechanisms behind precipitation and temperature to soil moisture variability and soil drying also have been investigated by means of qualitative analysis and quantitative contributions. This is important for deepening our understanding of regional drying and taking reasonable measures to improve the ecological environment and actively address climate change.

We organize the paper as follows: The data sets and the methods for analysis are described in section 2. In section 3, the analysis results are presented. A summary and discussion are provided in section 4.

## 2. Data Sets and Methods

We selected East Asia (20°N–55°N, 70°E–140°E) as the study region, which has experienced excessive warming and drying in recent years. The water scarcity here has been already a concern detected by precipitation, runoff, and other arid indices [*Li et al*., 2014; *Xu et al*., 2010], affected by natural reasons and human activities [*Ren et al*., 2002].

The data used here are the monthly GLDAS version 2 product (GLDAS-2) for the period of January 1948 to December 2010 with a spatial resolution of 1°×1° and the simulated monthly mean soil moisture of Coupled Model Intercomparison Project phase 5 (CMIP5).

### 2.1. GLDAS-2 Data

The GLDAS-2 product is a simulation output from the National Centers for Environmental Prediction/Oregon State University/Air Force/Hydrologic Research Laboratory (NOAH) [*Chen and Dudhia*, 2001; *Chen et al*., 1997, 1996; *Ek et al*., 2003; *Koren et al*., 1999] land-surface model, forced with the Princeton meteorological data set [*Sheffield et al*., 2006], which includes surface air temperature, precipitation (sum of rainfall and snowfall), and four layers of soil moisture content. The depths of the four soil layers range from 0 to 10, 10 to 40, 40 to 100, and 100 to 200 cm, and the units of soil moisture has been changed to volumetric ($m^3/m^3$). In view of the comparability in different layers, we use the mean soil moisture from 0 to 200 cm. GLDAS is a global, high-resolution, off-line land-surface simulation system, which was developed jointly by the National Aeronautics and Space Administration/Goddard Space Flight Center (NASA/GSFC) and the National Oceanographic and Atmospheric Administration/National Centers for Environmental Prediction (NOAA/NCEP). The goal was to generate optimal fields of land surface states and fluxes by integrating satellite- and ground-based observational data products, using land surface modeling and data assimilation techniques [*Rodell et al*., 2004]. The GLDAS data set was validated against available data from multiple sources [*Chen et al*., 2013; *Dorigo et al*., 2012; *Zhang et al*., 2008]. It is widely used, in terms of data assimilation, validation, weather and climate model initialization, and hydrology [*Lin et al*., 2008; *Reichle et al*., 2007; *Syed et al*., 2008].

### 2.2. CMIP5 Data

Because the soil layers of total soil moisture for different general circulation models (GCMs) of CMIP5 are different and the long-term variability of total soil moisture, we concerned in the paper, is similar to the top 10 cm layer. Thus, the simulated monthly mean soil moisture of CMIP5 used in this study is the mass of water in all phases in the top 10 cm layer ($kg/m^2$) [*Taylor et al*., 2012], and the units of soil moisture has been changed to volumetric ($m^3/m^3$). We used the outputs from 20 coupled general circulation models (CGCMs or climate models) with specified historical anthropogenic and natural external forcing and with 21st century changes in greenhouse gases and anthropogenic aerosols following the Representative Concentration Pathway (RCP) 8.5 and RCP4.5 simulation scenarios (Table 1). The first ensemble run was used if a model had multiple ensemble simulations. We choose the period of 1948 to 2005 of the historical experiment and 2006 to 2100 of the RCP experiment for our calculations and analyses.

### 2.3. Methods

The methods used in this paper include correlation analysis, regression analysis, moving *t* test, and the maximum covariance analysis (MCA). MCA, also known as singular value decomposition analysis, is a useful tool for detecting coupled patterns between two different geophysical fields, which is frequently used in climate research. By performing an eigenanalysis on the temporal covariance matrix between two data fields, MCA is able to isolate pairs of spatial patterns and their associated time series. To do so, MCA

**Table 1.** A List of CMIP5 General Circulation Models (GCMs) Used in This Study With a Brief Description[a]

| | Model Names | Origin |
|---|---|---|
| 1 | Beijing Climate Center–Climate System Model (BCC-CSM)1-1 | Beijing Climate Center, China |
| 2 | BCC-CSM1-1-m | Beijing Climate Center, China |
| 3 | Beijing Normal University-Earth System Model (ESM) | Beijing Normal University, China |
| 4 | Canadian Earth System Model version 2 | Canadian Centre for Climate, Canada |
| 5 | Community Climate System Model version 4 | National Center for Atmospheric Research, USA |
| 6 | Community Earth System Model, version 1–Biogeochemistry | National Center for Atmospheric Research, USA |
| 7 | Geophysical Fluid Dynamics Laboratory (GFDL) Climate Model version 3 | Geophysical Fluid Dynamics Laboratory, USA |
| 8 | GFDL-ESM2G | Geophysical Fluid Dynamics Laboratory, USA |
| 9 | GFDL-ESM2M | Geophysical Fluid Dynamics Laboratory, USA |
| 10 | Goddard Institute for Space Studies (GISS)-E2-H-CC | NASA Goddard Institute for Space Studies, USA |
| 11 | GISS-E2-R | NASA Goddard Institute for Space Studies, USA |
| 12 | GISS-E2-R-CC | NASA Goddard Institute for Space Studies, USA |
| 13 | Hadley Global Environment Model 2–Carbon Cycle | Met Office Hadley Centre, UK |
| 14 | HadGEM2-ES | Met Office Hadley Centre, UK |
| 15 | Institut Pierre-Simon Laplace (IPSL)-CM5A-LR | Institut Pierre-Simon Laplace, France |
| 16 | IPSL-CM5B-LR | Institut Pierre-Simon Laplace, France |
| 17 | Model for Interdisciplinary Research on Climate (MIROC) 5 | Atmosphere and Ocean Research Institute, Japan |
| 18 | MIROC-ESM | Japan Agency for Marine-Earth Science and Technology, Japan |
| 19 | MIROC-ESM-CHEM | Japan Agency for Marine-Earth Science and Technology, Japan |
| 20 | Meteorological Research Institute-CGCM3 | Meteorological Research Institute, Japan |

[a]The historical run (1948–2005) and two future scenario (RCP4.5 and RCP8.5) runs (2006–2100) from each model are used. The first ensemble run is used if a model has multiple ensemble runs.

extracts the coherent patterns of two variables that are most strongly related to each other [*Bretherton et al*., 1992]. Trends in this paper were calculated using the nonparametric Mann-Kendall test which has been widely used in detecting monotonic trends in hydrometeorological time series [*Dorigo et al*., 2012; *Sheffield and Wood*, 2008].

A method was adopted to study the contributions of temperature and precipitation to the soil moisture trend. First, a multiple linear regression is applied to obtain the soil moisture predictand regressed by annual mean precipitation and temperature fields at each grid point. The regression equation is shown as equation (1):

$$S' = a \times P + b \times T + C \tag{1}$$

in which $P$ and $T$ are the time series of annual mean precipitation and temperature, respectively; $a$ and $b$ are the regression coefficients; and $C$ is a constant. $S'$ is the soil moisture predictand, which can be roughly determined as the soil moisture component caused jointly by precipitation and temperature. This concept is widely used for separating the external and internal sea surface temperature trends [*Li et al*., 2011; *Polyakov et al*., 2010; *Ting et al*., 2009]. Similarly, the soil moisture component solely forced by precipitation (or temperature) can be obtained using a simple linear regression between soil moisture and precipitation (or temperature). Based on the multiple regression (equation (1)), the contributions of precipitation to the soil moisture trend (hereafter *CP*) can be calculated using equation (2):

$$CP = (a \times \Delta P)/\Delta S' \times 100\% \tag{2}$$

in which $\Delta S'$ and $\Delta P$ are the changes in mean $S'$ and precipitation between the first and last 10 years. Similarly, the contributions of temperature to soil moisture trend (hereafter CT) can be calculated using equation (3):

$$\mathrm{CT} = (b \times \Delta T)/\Delta S' \times 100\% \tag{3}$$

Notably, the contribution is relative, which means that the sum of CP and CT is equal to 100%.

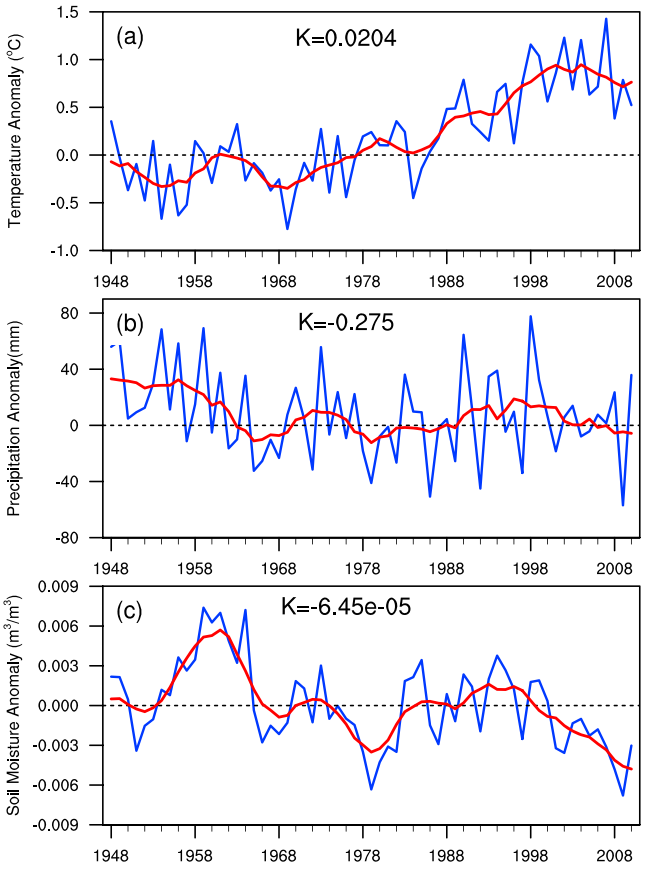


**Figure 1.** Annual mean (a) temperature, (b) precipitation, and (c) soil moisture anomaly of East Asia from 1948 to 2010 relative to 1961–1990 (blue curves), respectively. The red curves are the 7 year running mean and K is the trend calculated using the Mann-Kendall test.

## 3. Results

Over the past few decades, global warming and regional drying have been hot issues due to their major global implications. As one of the most sensitive areas to global changes, East Asia has been suffering significant warming and drying since the early 20th century [*Li and Ma*, 2013]. The annual mean temperature and precipitation anomaly over East Asia from 1948 to 2010 are plotted in Figures 1a and 1b. Rapid warming began in the early 1960s, and a hiatus has occurred since 2000, which coincides with the Northern Hemisphere mean temperature variation [*Wallace et al.*, 2012]. Comparing with temperature, the long-term variability of precipitation is not significant, despite a decreasing trend over the whole time span, with a rate of −2.75 mm/10 yr. It is noted that the precipitation decreased significantly before 1966 but has changed little since then. For example, the difference in precipitation for 2001 to 2010 relative to 1966 to 1976 is only 2.1 mm. Climate change associated with changes in precipitation and temperature would lead to changes in soil moisture. The time series of the annual mean soil moisture anomaly over East Asia (Figure 1c) shows an observable downward trend during the last 63 years with a rate of −0.000645 $m^3/m^3$/10 yr, which significantly exceeds the 95% confidence level. Within the long-term linear trends identified, considerable variability is observed at interannual to decadal time scales. The change in soil moisture demonstrates rapid drying in the early 1960s, an abrupt decrease around the mid-1960s, wetting from 1979 to 1993, and a resumption of drying in 1994. The abrupt change in soil moisture around the mid-1960s is significant, as determined by the moving *t* test. Before the mid-1960s, the soil moisture was ~0.249 $m^3/m^3$, whereas it decreased significantly to 0.239 $m^3/m^3$ after the shift in the mid-1960s.

Despite that the above analyses show obvious climate change in East Asia, the variability of which is spatially heterogeneous. Given this circumstance, further investigation of the spatial distribution of climate change over East Asia is necessary. The spatial distributions of annual mean temperature, precipitation, and soil moisture trends are shown in Figure 2. During the period of 1948 to 2010, most land areas have warmed by 1 to 3°C, with the warmest regions located over northern East Asia, especially north of 40°N (Figure 2a). Most of these warmest areas are arid and semiarid regions, which are characterized by low soil moisture, which is consistent with the results of recent studies from a global perspective [*Huang et al.*, 2012; *Ji et al.*, 2014]. During the same period, the decrease in precipitation seems distributed in a northeast-to-southwest belt, coinciding with the 600 mm precipitation line. As a result, 46% of East Asia revealed significant trend of soil moisture ($P = 0.05$) and mostly was decreasing (70%). The greatest drying occurred in northeast China, north China, part of Mongolia, and Russia near lake Baikal. In contrast, the most prominent wetting was in western China, being particularly pronounced over southern Xinjiang with a rate greater than 0.01 $m^3/m^3$/10 yr and significantly exceeding the 95% confidence level. The spatial distribution of the soil moisture trend resembles that of precipitation but with some regional differences. For example, the

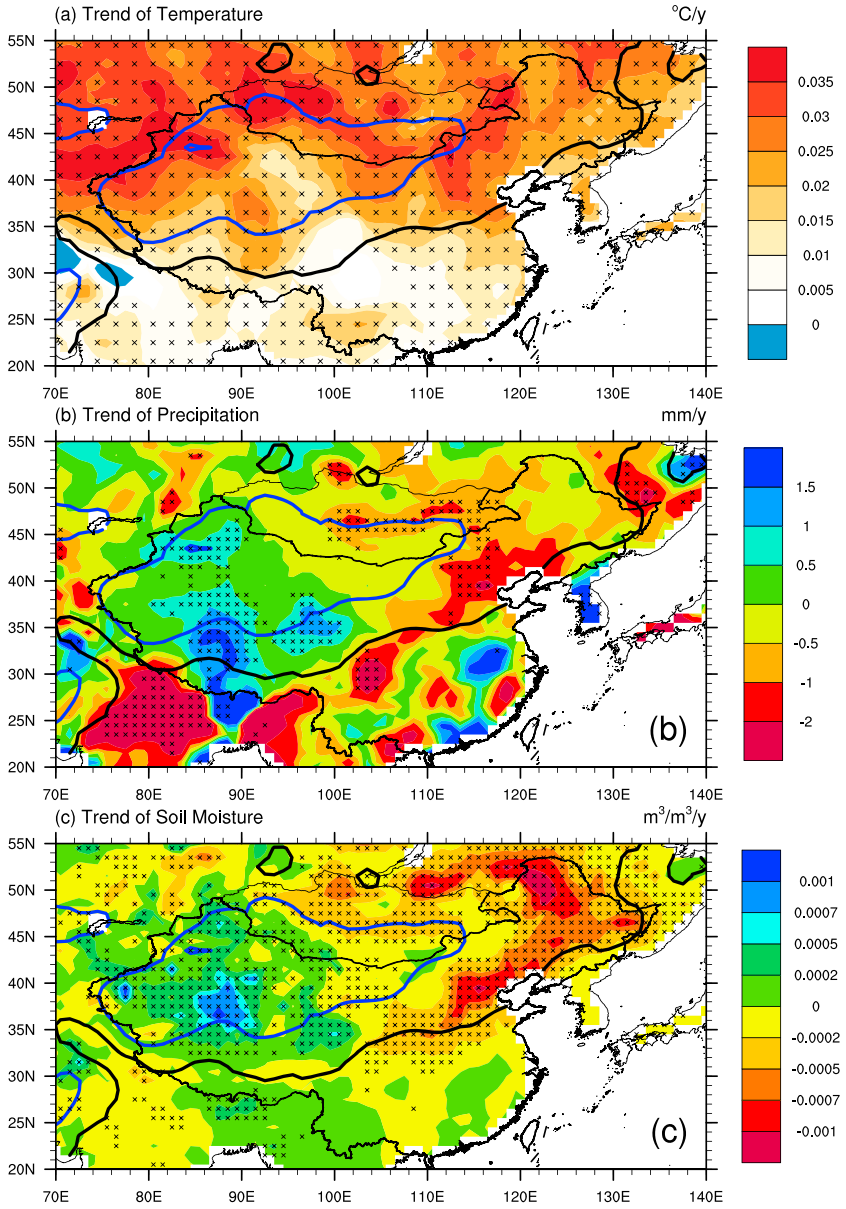


**Figure 2.** The spatial distribution of linear trend for annual mean (a) temperature, (b) precipitation, and (c) soil moisture from 1948 to 2010. The areas marked with crosses denote significant trends at the 95% confidence level according to a two-tailed Student's *t* test. The blue contour denotes 200 mm precipitation, and the black contour denotes 600 mm.

decrease in precipitation over Yunnan Province and southeastern India is significant, whereas soil drying is not significant and is even wetting. Inversely, severe soil drying near lake Baikal could not be revealed by the precipitation. This result indicates that the soil moisture depends largely on precipitation, but precipitation is not the only controlling factor. We note that the trend of soil moisture is broadly comparable with the drying characteristics revealed by various arid indices, such as the Palmer Drought Severity Index [*Dai*, 2011, 2013; *Wang et al*., 2014] and the Aridity Index [*Feng and Fu*, 2013], which suggest that the broad patterns exhibited by soil moisture data (Figure 2c) are likely reliable. The greatest variation occurs at intermediate moisture contents illustrated by Figure 2c and is consistent with observed soil moisture variation in temperate areas at short temporal and local scales [*Brocca et al*., 2012; *Lawrence and Hornberger*, 2007]. Lawrence et al. [*Lawrence and Hornberger*, 2007] provided a qualitative interpretation of variation peaks at intermediate moisture contents using a modified soil moisture dynamic model. In their interpretation, different behaviors in humid and arid catchments are related to different controlling

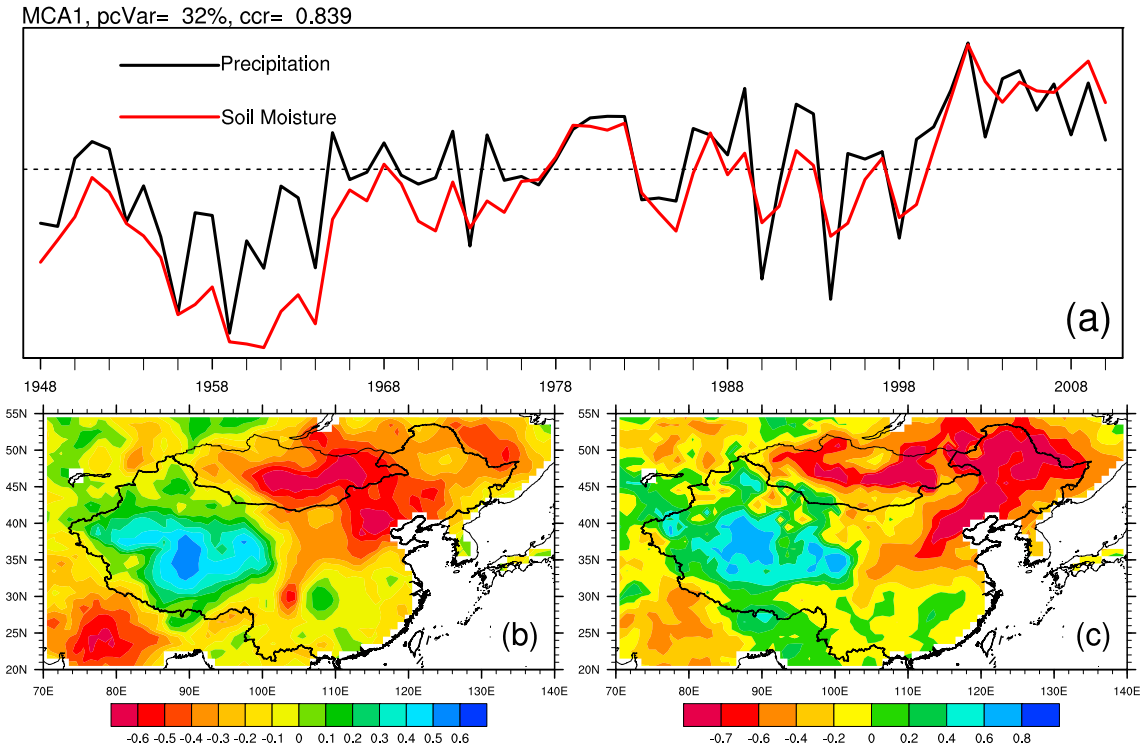


**Figure 3.** (a) Temporal and (b) spatial patterns of the MCA1 mode for precipitation and (c) soil moisture from 1948 to 2010 (normalized by its standard deviation prior to MCA analysis). The red (blue) areas are drying (wetting) for a positive temporal coefficient on the principal component (PC) time series. In Figure 3a, pcVar is the percentage variance explained by MCA1, and ccr is the correlation coefficient between PC1 precipitation and PC1 soil moisture, which is statistically significant at the 99% confidence level.

processes. Variance is controlled by the wilting point in arid areas, by soil conductivity in areas with intermediate moisture contents, and by porosity in humid areas. However, the physical mechanism was not provided in their paper.

Given the high changeability of soil moisture, analyzing the factors controlling soil moisture change is crucial for understanding the variability characteristics of soil moisture and taking effective measures to slow the rate of soil drying. Numerous environmental factors (such as soil texture, vegetation, and topography) and slight weather disturbance can lead to spatial and temporal variability in soil moisture. Interaction with the complex and nonlinear climate system complicates these processes. Intuitively, changes in precipitation will be the primary driver of variability in soil moisture, but it can also be modified by temperature changes. Here we carry out an MCA of precipitation and soil moisture for the period of 1948 to 2010. Figure 3 shows that the first leading MCA mode (MCA1) explains 32% of the variability in precipitation and soil moisture. This pattern represents the trends of precipitation and soil moisture that resemble those shown in its trend map (Figures 2b and 2c). We note that the spatial patterns of precipitation and soil moisture are similar, which suggest that the precipitation trend has a strong relationship with the long-term variability of soil moisture.

MCAs between temperature and soil moisture were also performed to identify the most remarkable temperature pattern on influencing soil moisture. Figure 4 shows that MCA1 patterns explain 75% of the total variance, which are the principal components. The temperature MCA1 patterns represent global warming, as the temporal coefficient is correlated strongly ($r = 0.96$) with the annual mean temperature (Figure 4a), and the spatial patterns (Figure 4b) resemble the warming patterns over East Asia (Figure 2a). Associated with this temperature mode, the soil moisture also exhibits similar temporal evolution (Figure 4a) but with particularly complex spatial patterns (Figure 4c) that resemble those shown on its trend map (Figure 2c). The soil moisture MCA1 patterns are positive in Mongolia, northeast China, and north China but negative in western East Asia. This result suggests that surface warming was also a crucial

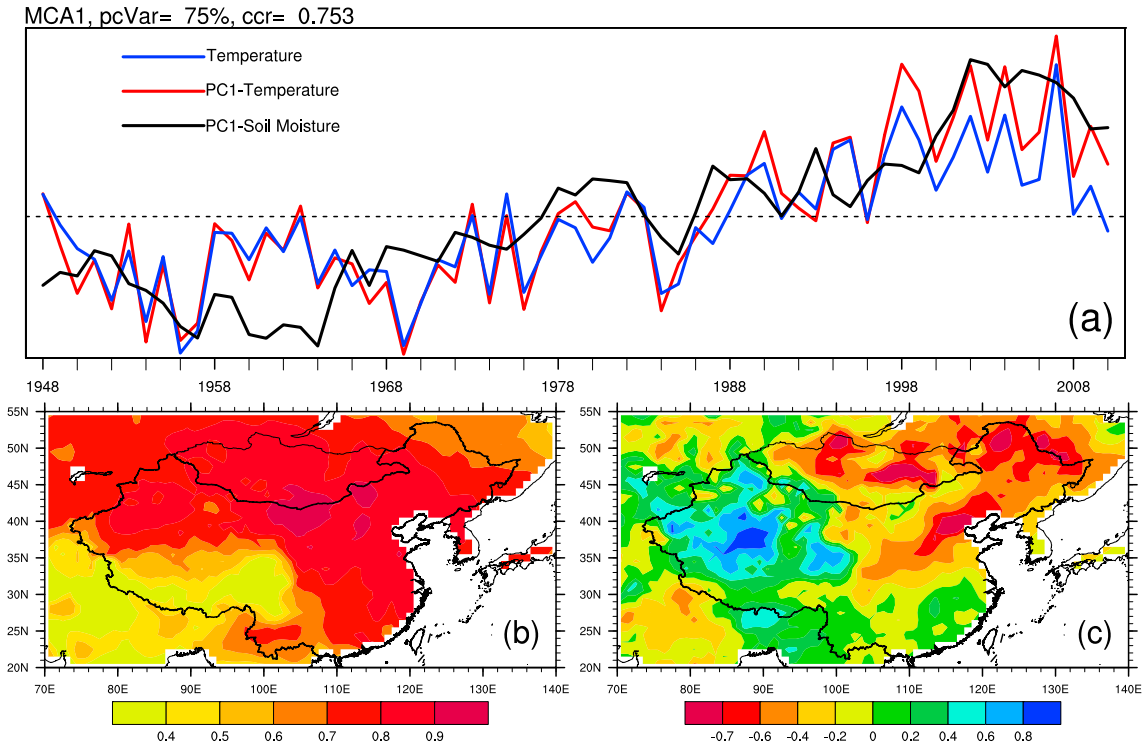


**Figure 4.** (a) Temporal and (b) spatial patterns of the MCA1 mode for temperature and (c) soil moisture from 1948 to 2010 (normalized by its standard deviation prior to MCA analysis). The red (blue) areas are drying (wetting) for a positive temporal coefficient on the PC time series. In Figure 4a, pcVar is the percentage variance explained by MCA1, and ccr is the correlation coefficient between PC1 temperature and PC1 soil moisture, which is statistically significant at the 99% confidence level. Also shown in Figure 4a is the area-mean temperature obtained from GLDAS (blue line). The correlation between area-mean temperature and PC1-temperature (PC1-soil moisture) time series is 0.96 (0.67), which is statistically significant at the 99% confidence level.

factor in the changes in the terrestrial water budget as well as precipitation. However, MCA cannot reveal the mechanisms between precipitation/temperature and soil moisture, so studies to determine the individual effects of precipitation and temperature on the soil moisture trend are warranted.

Figure 5 clearly shows the relationship of soil moisture with precipitation and temperature, which implies that changes in soil moisture can be partitioned into precipitation-induced and temperature-affected components. The role of precipitation as a driver of soil moisture trend is explicit. The precipitation trend controls the direction of soil moisture change, whether drying or wetting. As shown in Figure 5, most of the drying trend for soil moisture was located where precipitation decreases and the wetting trend where precipitation increases. This phenomenon is also appropriate for several other regions with diverse climates, such as central North America, West Africa, central Asia, and northern Europe [*Sheffield and Wood*, 2008]. However, the relationship between temperature trend (primarily temperature warming) and soil moisture wetting is somewhat unclear. In Figure 5 (right), the magnitude of the wetting trend is shown to be irregular compared with the temperature trend. We can

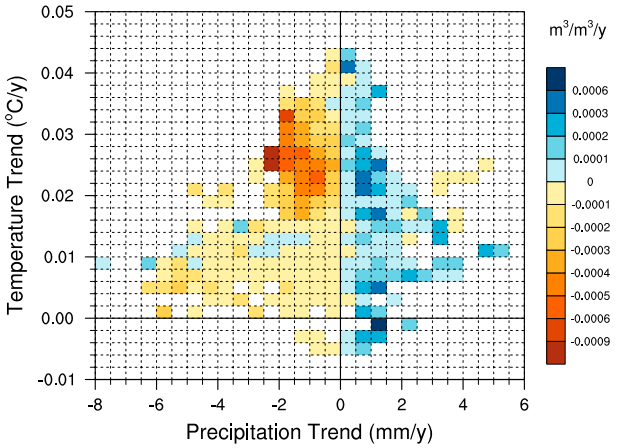


**Figure 5.** Trends of soil moisture as a function of precipitation and temperature trends. The colored boxes represent soil moisture trend. The red (blue) boxes are drying (wetting), and blank indicates no data. The unit of soil moisture trend is $m^3/m^3/yr$.

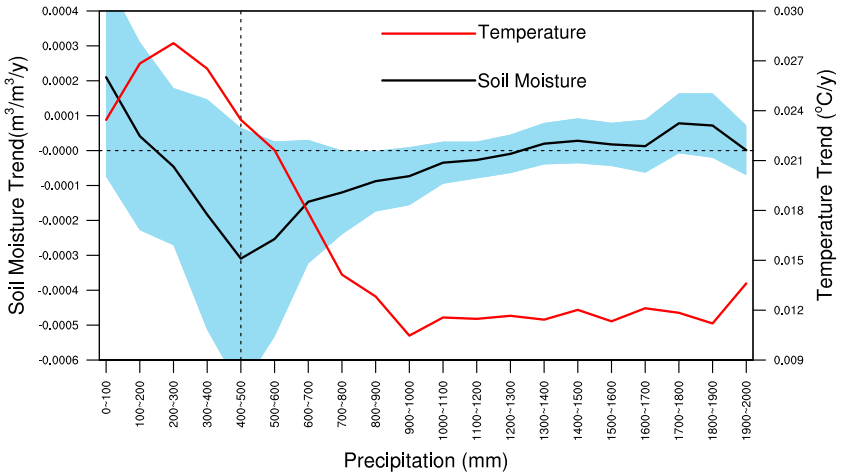


**Figure 6.** The linear trends of annual mean temperature and soil moisture as a function of climatological mean precipitation. The black line denotes the domain average for different climatic regions, and the shaded bands denote one standard deviation of the soil moisture trends. The climatological mean precipitation on the *x* axis is the annual mean precipitation for the period of 1961 to 1990.

only get the role of temperature warming as an amplifier on soil drying. Increasing temperature amplifies the effect of decreasing precipitation on soil drying. In Figure 5 (left), the magnitude of the drying trend at the top is shown to be larger than that at the bottom. This illustrates that soil drying is driven primarily by the lack of precipitation but is accentuated by associated increasing temperature. However, the enhancement of increasing temperature on soil drying is neither perfect nor unconditional. For example, the most obvious drying trend of soil moisture, when precipitation trend ranges from 0 to 1 mm/yr, occurs at intermediate temperature increases. This problem may be due to the manner of the influence of increasing temperatures on soil moisture change. Because temperature affects soil moisture through changing soil evapotranspiration, and temperature is not the only factor controlling evapotranspiration, the relationship between increasing temperature and soil moisture cannot be explicit. Generally speaking, evapotranspiration will increase with temperature warming, but it is not unlimited. If soil moisture is below a critical value, the soil suction will be so large that evapotranspiration will not increase. This is the soil moisture-limited or energy-limited evapotranspiration regime [*Seneviratne et al.*, 2010], which indicates the need for analysis of the increasing temperature-soil moisture relationship according to climatic region.

Figure 6 demonstrates the regionally averaged linear temperature and soil moisture trend as a function of climatological mean precipitation. The climatological mean precipitation is the annual mean precipitation for the period of 1961 to 1990, which represents the climatological state. It is also an intuitional representation of the spatial heterogeneity of temperature and soil moisture change shown in Figure 2. Temperature increases in semiarid regions with a warming peak around the precipitation range of 200 to 300 mm/yr. Corresponding to temperature warming, soil moisture also decreases markedly in semiarid regions, with the driest values in the range of 400 to 500 mm/yr. This result also reflects the discrepancy between the warmest and driest regions shown in Figure 5. However, of particular interest is the accordance after the precipitation range of 400 mm/yr, which is an energy-limited evapotranspiration regime. In this region, the magnitude of warming and drying decreases with the increase in precipitation. An obvious warming-drying trend arises in the intermediate moisture regions (precipitation ranging from 400 to 900 mm/yr), and the magnitude is quite small in the wet region (rainfall $>$ 1000 mm/yr). This result suggests that increased temperature would accentuate the drying caused by decreasing precipitation, at least in some regions.

Figure 7a shows the spatial distributions of the trends of the precipitation-forced soil moisture component. Comparing Figures 7a and 2c, we can see that the pattern of the precipitation component is remarkably similar to the total soil moisture trend. However, the magnitude is small in most areas of East Asia compared to the soil moisture trend, because the precipitation trend is not significant. Only Mongolia, north China, Bangladesh, and parts of northwest China show significant trends of precipitation-forced soil

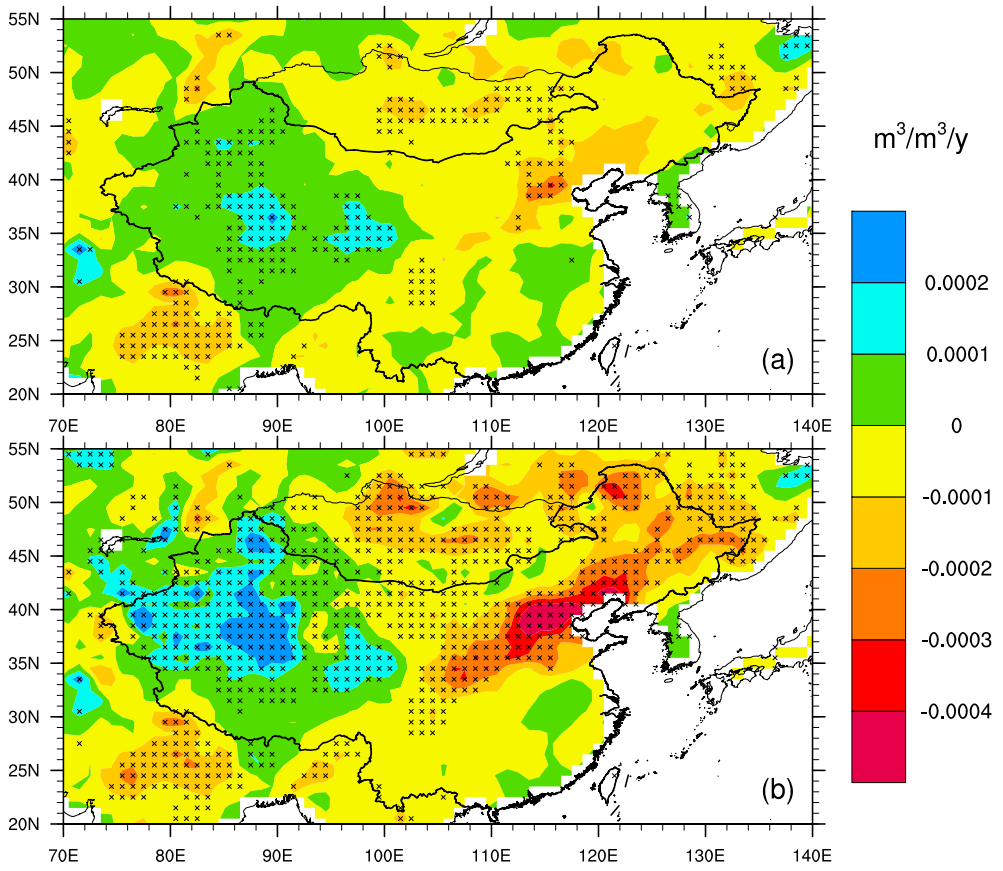


**Figure 7.** The spatial distribution of linear trend for soil moisture predictand linearly regressed by (a) precipitation and (b) precipitation and temperature. The areas marked with crosses denote significant trend at the 95% confidence level.

moisture component that are significant at the 95% confidence level. For the regions with negative soil moisture trend, only 14% present significant trends. The marked soil moisture trends illustrated in Figure 2 can be explained to some extent by temperature. Upon addition of temperature to the precipitation component, although the pattern of the soil moisture trend changes little, the magnitude becomes much more significant, especially in the north of China, where an observable increase in temperature has occurred. As shown in Figure 7b, more than 40% of the regions with soil moisture drying presented significant trends at the 95% confidence level, which reemphasizes the enhancement by increasing temperature of soil moisture drying, as mentioned earlier.

To express the quantitative effects of precipitation and temperature, their contributions are also calculated and illustrated in Figure 8. We focused on the mechanism of soil moisture drying in this study; therefore, regions with increasing soil moisture trends have been masked out. The results expressly represent the relative contributions of precipitation and temperature to soil moisture drying, which is spatially heterogeneous. In general, the contribution is dominated by precipitation over southern East Asia, by temperature over north China and northwestern East Asia, and the contributions of precipitation and temperature over East China are roughly equivalent. The averaged mean contribution of temperature for soil moisture drying over East Asia is about 58.1%, which is slightly larger than that of the precipitation (41.9%). That means increased temperature almost doubles the soil moisture drying caused by decreasing precipitation.

The qualitative analysis and quantitative contributions illustrate that temperature warming is an essential enhancement factor on soil drying caused by decreasing precipitation. The conclusion indicates that increased temperature would cause a more serious soil drying in the future, if the global warming that started in the 1960s persists. Model-predicted soil moisture change for the period of 2006 to 2100 is presented in Figure 9.

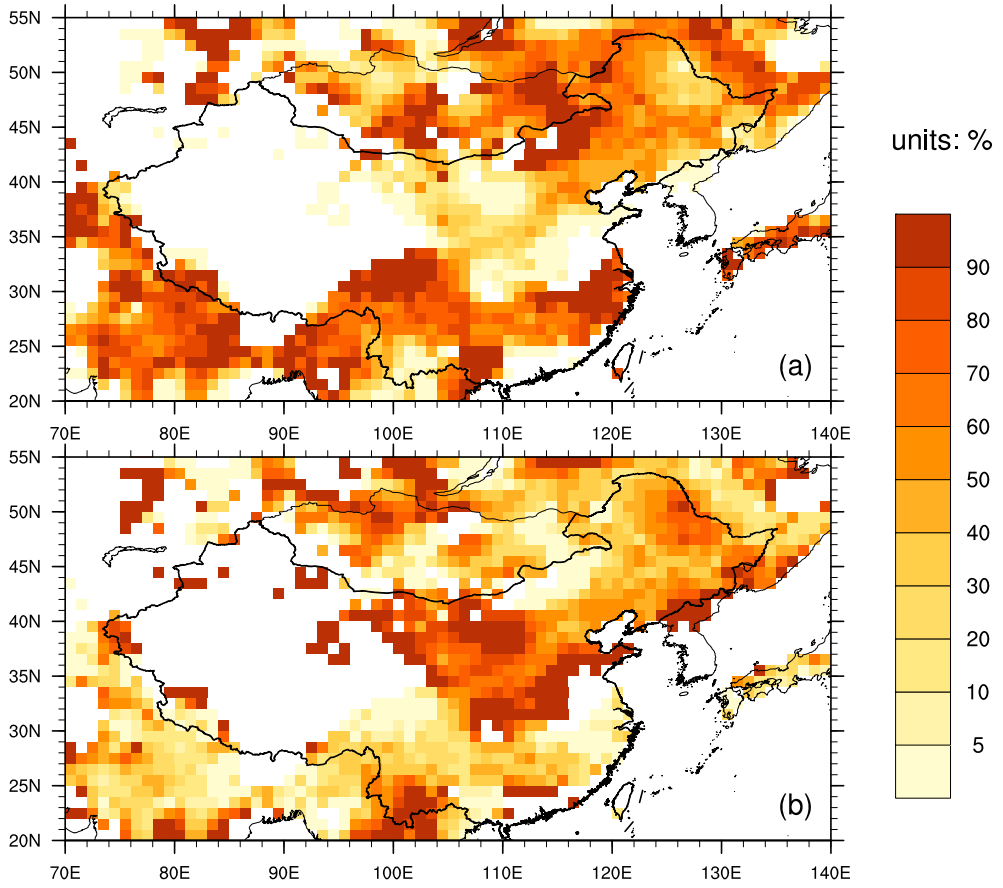


**Figure 8.** The relative contributions of (a) precipitation and (b) temperature to soil moisture trends. The relative contributions are calculated using equations (2) and (3) (see text and methods for more details). Regions with positive soil moisture change shown in Figure 7b have been masked out.

The results are based on the output from 20 models of CMIP5 following the RCP4.5 and RCP8.5 simulation scenarios. To compare the differences in soil moisture between GLDAS and CMIP5, the historical simulation of CMIP5 (black) and annual mean soil moisture anomalies of GLDAS for 0–10 cm are also shown. Because the internal variability in ensemble mean soil moisture has been removed, the GLDAS is the 20 year running mean.

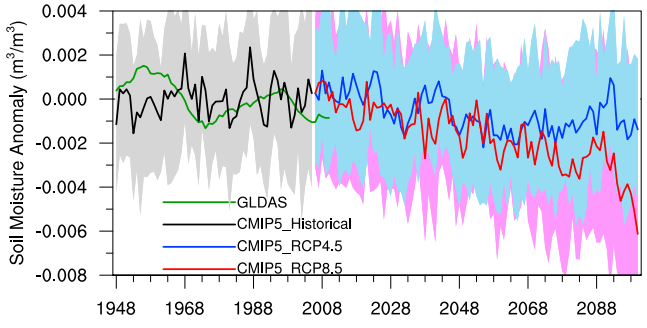


**Figure 9.** Annual mean soil moisture anomalies from the CMIP5 for RCP4.5 (blue), RCP8.5 (red), and for the historical simulation (black). The lines denote the ensemble mean of the 20 models, and the shaded bands denote one standard deviation of the multimodel response. The first ensemble run is used if a model has multiple ensemble runs. The soil moisture anomaly for the period of 1948 to 2010 from GLDAS is given in green for comparison. Because the internal variability of the ensemble-mean soil moisture has been removed, the GLDAS is the 20 year running mean.

Figure 9 shows that the ensemble mean of the 20 models is able to capture the variability of the GLDAS soil moisture from the early 1970s to the late 2000s. However, the model simulation is quite different from the GLDAS before the early 1970s, which could be the result of large natural variability, model deficiencies, and/or uncertainties in external forcing in the models. Despite the differences between the CMIP5 model and GLDAS, the models are able to simulate the robust downward trend of soil moisture following the early 1970s. The models also suggest a stronger trend in the 21st century from both RCP8.5 and RCP4.5 simulations than in the 20th century, followed by a

continued drying in RCP8.5, but with little change in RCP4.5 after the 2050s. The area-mean soil moisture in RCP8.5 (RCP4.5) is projected for 2071 to 2100 to decrease 0.00284 $m^3/m^3$ (0.00146 $m^3/m^3$), relative to 2006 to 2025, corresponding to relative decreases of 1.4% (0.7%). Climate models reflect a broad consensus that area-mean soil moisture will decrease in the 21st century: of the 20 models for RCP8.5 (RCP4.5), decreases are observed in 14 models, which comprise more than 70% of the models.

## 4. Summary and Discussion

Soil moisture is important to ecosystems, agriculture, and human activities. The change in soil moisture can extensively influence socioeconomics. This study used the GLDAS data to investigate the temporal and spatial characters of soil moisture variability over East Asia for the period of 1948 to 2010. It exhibited a clear, long-term decreasing trend of soil moisture over East Asia during the last several decades. However, the trend of soil moisture was spatially heterogeneous, with the most prominent wetting trend occurring over western East Asia and drying over northeast China, north China, part of Mongolia, and Russia near lake Baikal.

MCA analysis shows that the drying of soil moisture is notably related to global warming and decreasing precipitation. Nevertheless, the role of each individually differs. The role of decreasing precipitation is specific and is the primary factor driving the drying of soil moisture. However, the effect of increasing temperature on soil moisture trends depends largely on the climatic region. Over the precipitation range of 400 mm/yr, which is an energy-limited evapotranspiration regime, increasing temperature considerably amplifies the degree of soil drying caused by decreasing precipitation. The quantificational effect of temperature and precipitation on the soil moisture trend afforded by defining a contribution illustrates that increasing temperature almost doubles the soil moisture drying caused by decreasing precipitation, which is remarkably similar to the results of the qualitative analysis.

An aspect of our findings that requires special attention is that although the contributions of temperature and precipitation to the soil moisture trend were quantified using linear regression methods, the results, however, are not faultless because the climate system is complex and nonlinear. The use of linear regression methods on the complex and nonlinear climate system has several issues, especially when human activity is involved in the water cycle, which complicates the results and enhances the uncertainty. Even so, there is no doubt that increased temperature can lead to a decrease in soil moisture, as mentioned earlier. Following the RCP's simulation scenarios, the model-predicted soil moisture change for the period of 2006 to 2100 demonstrates a coincident decreasing trend across 20 climate models. To the end decade of the 21st century, the area-mean soil moisture is projected to decrease by 1.4% (0.7%) following the RCP8.5 (RCP4.5) simulation scenario, compared to that at the end of the 20th century.

Another aspect of our findings that needs to be discussed is that the data used in the paper are in essence from model products and the derived relationship may be affected by the modeling structure, despite that the GLDAS data were validated against various assimilation and observational data sets. In addition, temperature and precipitation are only two of the factors that control the variability of soil moisture, so they cannot account for all of the change. Other factors, such as soil texture, vegetation, topography, and human activities, are also important and even paramount in some cases [*Pan and Wang*, 2009]. The interaction between soil moisture and the Earth system has been the subject of much recent research. Besides, because soil drying is driven primarily by decreasing precipitation, thus the process which can affect the precipitation will be able to mitigate or enhance the soil drying, such as the poleward expansion of the Hadley circulation [*Lau and Kim*, 2015], which has become one of the hottest topics in climate change.

As mentioned above, increased temperature leads to an increase in evapotranspiration and a decrease in soil moisture. With decreasing soil moisture, the soil suction increases, the remaining soil moisture becomes less accessible for uptake by plant roots, and evapotranspiration may thus be reduced, possibly leading to an increase in sensible heat flux and a further temperature increase. The increased temperature, decreased evapotranspiration, and soil water loss form a positive feedback, and the strongest interaction appears in transitional zones between dry and wet climates [*Koster et al*., 2004; *Seneviratne et al*., 2010]. This positive feedback can continue until the soil is totally dry and desertification results, if the feedback loop is not broken up. This would destroy the ecological environment, depress crop production, and cause dust and drought.

This effect is most serious in the transitional regions due to three threats: severe drying, enhanced warming, and strongest interaction between increased temperature and decreased soil moisture. The strongest positive feedback between the most severe warming and drying will lead to dry land becoming even drier. Besides, the transitional regions are generally agricultural districts with large population. And the ecosystems are fragile and sensitive to climate change there; a slight disturbance in climate may be disastrous. The most serious warming and drying under recent and future would become a challenge to the ecosystem and human survival. Strict management and rational utilization of water resources are urgently needed to reduce the enormous influence of the recent and future drying.

**Acknowledgments**

We thank the World Climate Research Programme's Working Group on Coupled Modelling, the Global Organization for Earth System Science Portals for producing the CMIP5 model simulations and making them available for analysis, and the NASA/GSFC and NOAA/NCEP for producing and making available the GLDAS data set. The CMIP5 data sets for this paper are available at the ESGF peer-to-peer enterprise system (http://pcmdi9.llnl.gov). The GLDAS data sets are available at the Mirador data archive search interface (http://mirador.gsfc.nasa.gov/). Data Set name: GLDAS_NOAH10_M_020. This work was jointly supported by the National Basic Research Program of China (2012CB955301), the China 111 project (B13045), and the National Science Foundation of China (41305009). The English in this document has been checked by at least two professional editors, both native speakers of English. For a certificate, please see http://www.textcheck.com/certificate/gU8DZC.

## References

Bastiaanssen, W. (2000), SEBAL-based sensible and latent heat fluxes in the irrigated Gediz Basin, Turkey, *J. Hydrol.*, *229*(1), 87–100, doi:10.1016/S0022-1694(99)00202-4.

Bretherton, C. S., C. Smith, and J. M. Wallace (1992), An intercomparison of methods for finding coupled patterns in climate data, *J. Clim.*, *5*(6), 541–560, doi:10.1175/1520-0442(1992)005<0541:AIOMFF>2.0.CO;2.

Brocca, L., et al. (2011), Soil moisture estimation through ASCAT and AMSR-E sensors: An intercomparison and validation study across Europe, *Remote Sens. Environ.*, *115*(12), 3390–3408, doi:10.1016/j.rse.2011.08.003.

Brocca, L., T. Tullo, F. Melone, T. Moramarco, and R. Morbidelli (2012), Catchment scale soil moisture spatial–temporal variability, *J. Hydrol.*, *422*, 63–75, doi:10.1016/j.jhydrol.2011.12.039.

Chen, F., and J. Dudhia (2001), Coupling an advanced land surface-hydrology model with the Penn State-NCAR MM5 modeling system. Part I: Model implementation and sensitivity, *Mon. Weather Rev.*, *129*(4), 569–585, doi:10.1175/1520-0493(2001)129<0569:CAALSH>2.0.CO;2.

Chen, F., K. Mitchell, J. Schaake, Y. Xue, H. Pan, V. Koren, Q. Duan, M. Ek, and A. Betts (1996), Modeling of land surface evaporation by four schemes and comparison with FIFE observations, *J. Geophys. Res.*, *101*(D3), 7251–7268, doi:10.1029/95JD02165.

Chen, F., Z. Janjić, and K. Mitchell (1997), Impact of atmospheric surface-layer parameterizations in the new land-surface scheme of the NCEP mesoscale Eta model, *Boundary Layer Meteorol*, *85*(3), 391–421, doi:10.1023/A:1000531001463.

Chen, Y., K. Yang, J. Qin, L. Zhao, W. Tang, and M. Han (2013), Evaluation of AMSR-E retrievals and GLDAS simulations against observations of a soil moisture network on the central Tibetan Plateau, *J. Geophys. Res. Atmos.*, *118*, 4466–4475, doi:10.1002/jgrd.50301.

Ciais, P., et al. (2005), Europe-wide reduction in primary productivity caused by the heat and drought in 2003, *Nature*, *437*(7058), 529–533, doi:10.1038/nature03972.

Dai, A. (2011), Drought under global warming: A review, *WIRES Clim. Change*, *2*(1), 45–65, doi:10.1002/wcc.81.

Dai, A. (2013), Increasing drought under global warming in observations and models, *Nat. Clim. Change*, *3*(1), 52–58, doi:10.1038/nclimate1633.

Dorigo, W., R. Jeu, D. Chung, R. Parinussa, Y. Liu, W. Wagner, and D. Fernández-Prieto (2012), Evaluating global trends (1988–2010) in harmonized multi-satellite surface soil moisture, *Geophys. Res. Lett.*, *39*, L18405, doi:10.1029/2012GL052988.

Ek, M., K. Mitchell, Y. Lin, E. Rogers, P. Grunmann, V. Koren, G. Gayno, and J. Tarpley (2003), Implementation of Noah land surface model advances in the National Centers for Environmental Prediction operational mesoscale Eta model, *J. Geophys. Res.*, *108*(D22), 8851, doi:10.1029/2002JD003296.

Feng, S., and Q. Fu (2013), Expansion of global drylands under a warming climate, *Atmos. Chem. Phys.*, *13*(19), 10,081–10,094, doi:10.5194/acp-13-10081-2013.

Fierer, N., and J. P. Schimel (2002), Effects of drying–rewetting frequency on soil carbon and nitrogen transformations, *Soil Biol. Biochem.*, *34*(6), 777–787, doi:10.1016/S0038-0717(02)00007-X.

Granier, A., et al. (2007), Evidence for soil water control on carbon and water dynamics in European forests during the extremely dry year: 2003, *Agric. Forest Meteorol.*, *143*(1), 123–145, doi:10.1016/j.agrformet.2006.12.004.

Guan, X., J. Huang, N. Guo, J. Bi, and G. Wang (2009), Variability of soil moisture and its relationship with surface albedo and soil thermal parameters over the Loess Plateau, *Adv. Atmos. Sci.*, *26*(4), 692–700, doi:10.1007/s00376-009-8198-0.

Hohenegger, C., P. Brockhaus, C. S. Bretherton, and C. Schär (2009), The soil moisture–precipitation feedback in simulations with explicit and parameterized convection, *J. Clim.*, *22*(19), 5003–5020, doi:10.1175/2009JCLI2604.1.

Huang, J., W. Zhang, J. Zuo, J. Bi, J. Shi, X. Wang, Z. Chang, Z. Huang, S. Yang, and B. Zhang (2008), An overview of the semi-arid climate and environment research observatory over the Loess Plateau, *Adv. Atmos. Sci.*, *25*(6), 906–921, doi:10.1007/s00376-008-0906-7.

Huang, J., P. Minnis, H. Yan, Y. Yi, B. Chen, L. Zhang, and J. K. Ayers (2010), Dust aerosol effect on semi-arid climate over northwest China detected from A-Train satellite measurements, *Atmos. Chem. Phys.*, *10*(14), 6863–6872, doi:10.5194/acp-10-6863-2010.

Huang, J., X. Guan, and F. Ji (2012), Enhanced cold-season warming in semi-arid regions, *Atmos. Chem. Phys.*, *12*(12), 5391–5398, doi:10.5194/acp-12-5391-2012.

Huang, J., T. Wang, W. Wang, Z. Li, and H. Yan (2014), Climate effects of dust aerosols over East Asian arid and semiarid regions, *J. Geophys. Res. Atmos.*, *119*, 11,398–11,416, doi:10.1002/2014JD021796.

Ji, F., Z. Wu, J. Huang, and E. P. Chassignet (2014), Evolution of land surface air temperature trend, *Nat. Clim. Change*, *4*, 462–466, doi:10.1038/nclimate2223.

Koren, V., J. Schaake, K. Mitchell, Q. Duan, F. Chen, and J. Baker (1999), A parameterization of snowpack and frozen ground intended for NCEP weather and climate models, *J. Geophys. Res.*, *104*(D16), 19,569–19,585, doi:10.1029/1999JD900232.

Koster, R., P. Dirmeyer, Z. Guo, G. Bonan, E. Chan, P. Cox, C. Gordon, S. Kanae, E. Kowalczyk, and D. Lawrence (2004), Regions of strong coupling between soil moisture and precipitation, *Science*, *305*(5687), 1138–1140, doi:10.1126/science.1100217.

Lau, W., and K. Kim (2015), Robust Hadley circulation changes and increasing global dryness due to $CO_2$ warming from CMIP5 model projections, *Proc. Natl. Acad. Sci. U.S.A.*, *112*(12), 3630–3635, doi:10.1073/pnas.1418682112s.

Lawrence, J. E., and G. M. Hornberger (2007), Soil moisture variability across climate zones, *Geophys. Res. Lett.*, *34*, L20402, doi:10.1029/2007GL031382.

Li, G., B. Ren, J. Zheng, and C. Yang (2011), Net air–sea surface heat flux during 1984–2004 over the North Pacific and North Atlantic Oceans (10°N–50°N): Annual mean climatology and trend, *Theor. Appl. Climatol.*, *104*(3–4), 387–401, doi:10.1007/s00704-010-0351-2.

Li, M., and Z. Ma (2013), Soil moisture-based study of the variability of dry-wet climate and climate zones in China, *Chin. Sci. Bull.*, *58*(4–5), 531–544, doi:10.1007/s11434-012-5428-0.

Li, Y., J. Huang, M. Ji, and J. Ran (2014), Dryland expansion in northern China from 1948 to 2008, *Adv. Atmos. Sci.*, *32*(6), 870–876, doi:10.1007/s00376-014-4106-3.
Lin, B., P. W. Stackhouse, P. Minnis, B. A. Wielicki, Y. Hu, W. Sun, T. F. Fan, and L. M. Hinkelman (2008), Assessment of global annual atmospheric energy balance from satellite observations, *J. Geophys. Res.*, *113*, D16114, doi:10.1029/2008JD009869.
Nakshabandi, G. A., and H. Kohnke (1965), Thermal conductivity and diffusivity of soils as related to moisture tension and other physical properties, *Agric. Meteorol.*, *2*(4), 271–279, doi:10.1016/0002-1571(65)90013-0.
Pan, Y., and X. Wang (2009), Factors controlling the spatial variability of surface soil moisture within revegetated-stabilized desert ecosystems of the Tengger Desert, northern China, *Hydrol. Processes*, *23*(11), 1591–1601, doi:10.1002/hyp.7287.
Polyakov, I. V., V. A. Alexeev, U. S. Bhatt, E. I. Polyakova, and X. Zhang (2010), North Atlantic warming: Patterns of long-term trend and multidecadal variability, *Clim. Dyn.*, *34*(2–3), 439–457, doi:10.1007/s00382-008-0522-3.
Reichle, R. H., R. D. Koster, P. Liu, S. P. Mahanama, E. G. Njoku, and M. Owe (2007), Comparison and assimilation of global soil moisture retrievals from the Advanced Microwave Scanning Radiometer for the Earth Observing System (AMSR-E) and the Scanning Multichannel Microwave Radiometer (SMMR), *J. Geophys. Res.*, *112*, D09108, doi:10.1029/2006JD008033.
Reichstein, M., et al. (2007), Reduction of ecosystem productivity and respiration during the European summer 2003 climate anomaly: A joint flux tower, remote sensing and modelling analysis, *Global. Change Biol.*, *13*(3), 634–651, doi:10.1111/j.1365-2486.2006.01224.x.
Ren, L., M. Wang, C. Li, and W. Zhang (2002), Impacts of human activity on river runoff in the northern area of China, *J. Hydrol.*, *261*(1), 204–217, doi:10.1016/S0022-1694(02)00008-2.
Rodell, M., et al. (2004), The Global Land Data Assimilation System, *Bull. Am. Meteorol. Soc.*, *85*(3), 381–394, doi:10.1175/BAMS-85-3-381.
Seneviratne, S. I., T. Corti, E. L. Davin, M. Hirschi, E. B. Jaeger, I. Lehner, B. Orlowsky, and A. J. Teuling (2010), Investigating soil moisture–climate interactions in a changing climate: A review, *Earth Sci. Rev.*, *99*(3), 125–161, doi:10.1016/j.earscirev.2010.02.004.
Sheffield, J., and E. F. Wood (2008), Global trends and variability in soil moisture and drought characteristics, 1950–2000, from observation-driven simulations of the terrestrial hydrologic cycle, *J. Clim.*, *21*(3), 432–458, doi:10.1175/2007JCLI1822.1.
Sheffield, J., G. Goteti, and E. Wood (2006), Development of a 50-year high-resolution global dataset of meteorological forcings for land surface modeling, *J. Clim.*, *19*(13), 3088–3111, doi:10.1175/JCLI3790.1.
Syed, T., J. Famiglietti, M. Rodell, J. Chen, and C. Wilson (2008), Analysis of terrestrial water storage changes from GRACE and GLDAS, *Water Resour. Res.*, *44*, W02433, doi:10.1029/2006WR005779.
Taylor, K. E., R. J. Stouffer, and G. A. Meehl (2012), An overview of CMIP5 and the experiment design, *Bull. Am. Meteorol. Soc.*, *93*(4), 485–498, doi:10.1175/BAMS-D-11-00094.1.
Teuling, A. J., and S. I. Seneviratne (2008), Contrasting spectral changes limit albedo impact on land-atmosphere coupling during the 2003 European heat wave, *Geophys. Res. Lett.*, *35*, L03401, doi:10.1029/2007GL032778.
Ting, M., Y. Kushnir, R. Seager, and C. Li (2009), Forced and internal twentieth-century SST trends in the North Atlantic, *J. Clim.*, *22*(6), 1469–1481, doi:10.1175/2008JCLI2561.1.
Wallace, J. M., Q. Fu, B. V. Smoliak, P. Lin, and C. M. Johanson (2012), Simulated versus observed patterns of warming over the extratropical Northern Hemisphere continents during the cold season, *Proc. Natl. Acad. Sci. U.S.A.*, *109*(36), 14,337–14,342, doi:10.1073/pnas.1204875109.
Wang, G., J. Huang, W. Guo, J. Zuo, J. Wang, J. Bi, Z. Huang, and J. Shi (2010), Observation analysis of land-atmosphere interactions over the Loess Plateau of northwest China, *J. Geophys. Res.*, *115*, D00K17, doi:10.1029/2009JD013372.
Wang, S., J. Huang, Y. He, and Y. Guan (2014), Combined effects of the Pacific Decadal Oscillation and El Niño–Southern Oscillation on global land dry–wet changes, *Sci. Rep.*, *4*, 6651, doi:10.1038/srep06651.
Wetzel, P. J., and J. T. Chang (1987), Concerning the relationship between evapotranspiration and soil moisture, *J. Clim. Appl. Meteorol.*, *26*(1), 18–27, doi:10.1175/1520-0450(1987)026<0018:CTRBEA>2.0.CO;2.
Xu, K., J. Milliman, and H. Xu (2010), Temporal trend of precipitation and runoff in major Chinese Rivers since 1951, *Global Planet. Change*, *73*(3), 219–232, doi:10.1016/j.gloplacha.2010.07.002.
Yang, K., T. Watanabe, T. Koike, X. Li, H. Fujii, K. Tamagawa, Y. Ma, and H. Ishikawa (2007), Auto-calibration system developed to assimilate AMSR-E data into a land surface model for estimating soil moisture and the surface energy budget, *J. Meteorol. Soc. Jpn.*, *85A*, 229–242.
Yang, K., T. Koike, I. Kaihotsu, and J. Qin (2009), Validation of a dual-pass microwave land data assimilation system for estimating surface soil moisture in semiarid regions, *J. Hydrometeorol.*, *10*(3), 780–793, doi:10.1175/2008JHM1065.1.
Yang, Z., et al. (2011), The community Noah land surface model with multiparameterization options (Noah-MP): 2. Evaluation over global river basins, *J. Geophys. Res.*, *116*, D12110, doi:10.1029/2010JD015140.
Zhang, J., W. C. Wang, and J. Wei (2008), Assessing land-atmosphere coupling using soil moisture from the Global Land Data Assimilation System and observational precipitation, *J. Geophys. Res.*, *113*, D17119, doi:10.1029/2008JD009807.